International Journal of Thin Films Science and Technology

http://dx.doi.org/10.18576/ijtfst/110116

Electrical and Optical Properties of Flexible Transparent Silver Nanowires electrodes

Rabeea D. Abdel-Rahim, Adham M. Nagiub and Mahmoud A. Taher*

Chemistry Department, Faculty of Science, Al-Azhar University, Assiut 71524, Egypt

Received: 22 Aug. 2021, Revised: 3 Dec. 2021, Accepted: 9 Dec. 2021

Published online:1 Jan. 2022

Abstract: AgNWs were produced by the one-pot polyol method, and it had been produced by reduction of $AgNO_3$ by ethylene glycol in presence of polyvinylpyrrolidone (PVP) and KCl at high temperature of about 160 ºC. AgNWs suspension were purified by centrifuging at 3000 rpm for three times then re-depressed in deionized water with a concentration of 1%. The purified suspension was diluted to different concentrations (2-5) mg. mL^{-1} using 1% of hydroxy methylcellulose to design different AgNWs transparent conductive films (AgNWs-TCFs). AgNWs suspension inks were coated on the glass and polyethylene terephthalate (PET) substrates. Different AgNWs diameters were obtained by changing the synthesis conditions. It has been observed that the wire diameter will greatly affect both the optical and electrical properties of the obtained AgNWs-TCFs. The best obtained AgNWs-TCFs had high transparency of about 91.5 %, small sheet resistance of about 14 .03 Ω and optical haze less than 2%, which met the requirements for the manufacture of optoelectronic and sensor equipment.

Keywords: Silver nanowires, transparent conductive electrode, flexible electrodes, polyol method, AgNWs size control, AgNWs size-dependent and one-pot synthesis.

1. Introduction

Flexible transparent conductive film (FTCF) is now an important part of many flexible electronic devices. (FTCF) based on the silver nanowire (AgNWs) network has received widespread attention due to its comprehensive optoelectronic properties and is expected to become a new generation of transparent conductive film materials. Due to the simplicity of production and processing, printed electronics technology has become a popular method for producing low-cost, high-quality flexible electronic devices. Transparent conductive electrodes are the fundamental components of touch screens, light-emitting diodes, smart windows, and solar cells[1-3]. Because it is extremely conductive and transparent, indium doped in tin oxide (ITO) is the main material of choice for transparent conducting films in flat-panel displays, organic solar cells, and organic light-emitting diodes[3, 4]. It has a sheet resistance of 10 ohm/sq at a transmittance of 90% (λ= 550 nm). However, indium is a rare material, fragile, expensive and requires a vapor coating process for its production that is 1,000 times slower than newspaper printing.[5]. These issues have prompted a quest a lot of researchers for flexible ITO replacements that can be deposited from liquids at high coating speeds. The alternative materials which been studied such as conductive polymers (CP) poly(3,4-ethylene dioxythiophene)poly(styrenesulfonate) [6-8], carbon nanotubes (CNT) [9], polymer-metal hybrid transparent electrode[10, 11], metals nanowires (MNWs) [12], Cupper nanowires,[13-15], films of silver nanowires AgNWs currently have the highest transmittance and a high conductance [16-19].

Recently, Silver nanowires are used in many modern and important applications such as solar cells [20], flexible electronic devices [21], touch screen panels [22], electrochromic devices [23], supercapacitors [24], electromagnetic interference (EMI) shielding materials [25] and conductive electrodes [26]. AgNWs is a one-dimensional linear material with a high aspect ratio (length to diameter ratio), which is directly related to its production technique. Moreover, flexible conductors are not only used in electronic fields but have been widely used in biological fields[27], water splitting bifunctional electrocatalysts[28] and dye degradation [29]. Based on this, it is worth mentioning the research and development in the design of

*Corresponding author E-mail: adham.nagiub@azhar.edu.eg

flexible electrodes and AgNWs are one of the most common materials used in designing of flexible electrodes.

So far, a lot of methods have been applied to synthesize AgNWs and to improve the morphological structure. Hydrothermal [30], DNA templates [31], wet chemical synthesis [32], electrochemical [33] and polyol method[31] are the main methods used. In terms of low cost, high aspect ratio and controllability of morphological structure, polyol technology is the most impressive method for synthesizing silver nanowires. This reaction had been done by heating via the reduction of a metal salt by a polyol in presence of poly(vinylpyrrolidone) (PVP). The first preparation of nanoparticles by polyol process had been done by F. Fievet et al., in 1989 [34]. A lot of researchers have modified this technique to simplify the synthesize AgNWs with different morphologies and high aspect ratio [35-38].

Herein, synthesis of AgNWs with a high aspect ratio of more than 1700 had been done successfully by the one-step polyol method, the produced AgNWs ink was purified and formulated to be coated on different substrates. The optical and electrical properties were calculated for different AgNWs-TCFs.

2. Materials and methods:

All chemicals with high-quality analytical-grade products (Silver nitrate ($AgNO_3$), polyvinylpyrrolidone (PVP) (Mo. Wt. 40,000), glycerol and KCl) were purchased from Sigma Aldrich and used without further purification.

2.1 Synthesis of AgNWs:

Silver nanowires were synthesized in one step polyol method [39]. 10 milliliters of Ethylene glycol (EG), 5 milliliters of KCl (0.005 grams of KCl in 5 milliliters of EG), 0.3 grams of PVP solution (50 percent in EG), and 0.15 g $AgNO_3$ were mixed in one container. The temperature adjusted to 160 °C. Following that, the temperature is maintained at 160 °C until the appearance of AgNWs with the desired gray color then the reaction was stopped by using an ice bath. The AgNWs product was cleaned by centrifuge at 2000-3000 rpm according to the size of the wires three times, then re-dispersed in deionized water. Different AgNWs were obtained by changing the reaction conditions [40, 41].

2.2 Electrodes designing:

1% AgNWs suspension is re-dispersed well-using sonicator for 10 minutes. Using 0.1% by weight of hydroxy methylcellulose as a thickener, the AgNWs were made into the formulated AgNWs ink, the dispersed AgNWs suspension was then diluted to from 2 $mg.mL^{-1}$ to 5 $mg.mL^{-1}$. The final AgNWs suspension (ink) was then coated by using a spin coater at 3500 rpm for 45 seconds on a clean glass substrate. The flexible AgNWs transparent electrodes were prepared by coating AgNWs on a polyethylene terephthalate (PET). Firstly, PET is immersed in hydrogen peroxide for 2 hours to make it hydrophilic, and then washed with ethanol several times. The coating of AgNWs on the pretreated PET was done by using of Meyer rods.

2.3 Morphological characterization

Scanning electron microscope (SEM) images were captured using a Joel (Tokyo, Japan) JSM 5600 LV scanning electron microscope equipped with Oxford Instruments 6587 EDX microanalysis detector, and X-ray diffraction (XRD) Spectro-ray diffractometer was obtained using a Philips PW 1710 (Japan) V-530 X (Cu; K radiation at 40.1V and 30mA, = 0.154 nm). UV-Vi spectrum analysis has been performed by using JASCO Model V-530 (Japan).

3. Result and dissuasion

A typical synthesis of AgNWs according to polyol method in which glycerol is used as a both a solvent and a reducing agent at a high temperature of about 160ºC can be represented according to the following chemical equations:

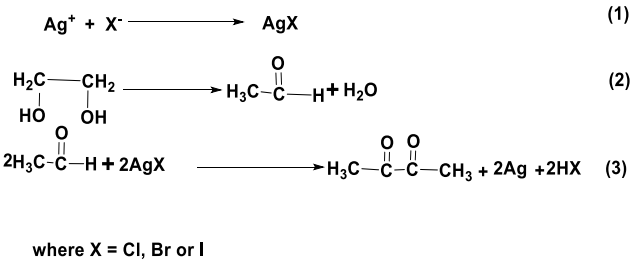

equation (1) describes the first step in AgNWs synthesis, that takes place by reacting Ag^+ cations with chloride anions to produce AgCl. Chloride anions play two important roles in the synthesis of AgNWs by enhancing the decrease of Ag^+ and can regulate the silver concentration[38, 42] and act as a capping agent beside PVP that will passivates the (100) plane and help the crystal growth in the (111) plane[43]. According to equations 2 and 3, the formation of Ag atoms (seeds) by reducing Ag^+ cations with EG. Furthermore, the concentration of the seeds will reach the level of supersaturation, where the nucleation of Ag atoms will occur and begin to develop into silver nanostructures[44, 45].

PVP has a high tendency to form coordination bonds with several chemical compounds. the skeleton of PVP which has a strong polar group (pyrrolidone ring) leads to the ability to coordinate with many chemical compounds. PVP plays a fundamental role in the arrangement of Ag^+ cations by the adsorption of Ag^+ cations on its surface. Carbonyl polar groups(C=O) act as active sites that can coordinate with Ag^+ ions to form the PVP-Ag complex that will be reduced to PVP-Ag^+ to form AgNWs nuclei [42] (scheme 1).

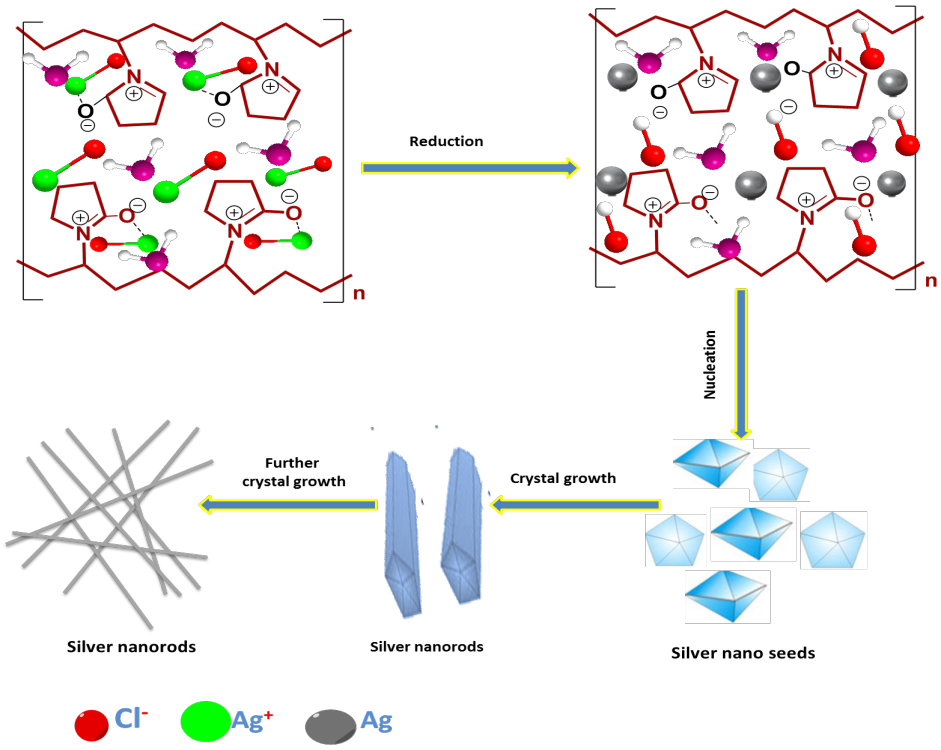

Scheme 1. Silver nanowires growth mechanism.

If excess amount of PVP were used no AgNWs will be formed because PVP will bind to all crystal faces of Ag crystalline structure which will lead to the formation of AgNPs [44, 45].

3.1 X-ray diffraction (XRD): -

Fig.1 shows The XRD pattern to examine the films of AgNWs with different diameters coated on glass substrates. The XRD data obtained were treated with the Malvern Analytical software (X-Pert high score plus). XRD data indicates that the crystals of the synthesized AgNWs have a high crystalline structure. XRD data were fitted with JCPDS No. 98-018-0878 and it showed a cubic crystalline structure [46] (Fig. 1a). Also, XRD reveals five distinguished characteristic patterns at 38.37°, 44.6°, 64.91°, 77.991°and 82.18°, which are crossponding to face-centered cubic (FCC) (111), (200), (220), (311), and (222) planes, respectively. The crystal lattice structure constant was observed to be 4.0861, in agreement with the standard reported value of 4.0862 [37, 47, 48]. Moreover, The XRD data obtained refers to crystal lattice (d) spacing values of 2.31 A° and 2.14 A° for AgNWs, crossponding to planes (1 1 1) and (2 0 0), respectively. These results suggested that, high purity crystalline structures of AgNWs samples were produced successfully [49]. Furthermore, the ratio of intensity between (111) and (200) peaks showed a high value of 3.5 compared to the theoretical value of 2.5 that may suggest the enhancement of (111) crystalline planes in the AgNWs [42].

Fig. 1(b,c) exhibits XRD patterns of AgNWs samples with different average diameters of 16.87nm, 42.67 nm, 66.5nm and 105.4 nm, respectively. As was expected, XRD patterns for various AgNWs diameters emerged at approximately the same position but with varying intensities. The values of crystalline dimension (L_{ave}) for different AgNWs were computed according to the Scherrer equation (1) [47].

$$L_{ave} = \frac{K\lambda}{\beta cos\theta} \qquad (4)$$

where K is a dimensionless shape factor and the common standard value approximately 0.9, λ is the X-ray wavelength, β is the line broadening at full width at half maximum (FWHM) and θ is the Bragg's angle. The calculate (L_{ave}) of AgNWs with different diameters were shown in table 1. These values were observed to increase with increasing of the average AgNWs diameter. Fig. 1(d) shows the Amplification of (111) scattering peaks of AgNWs with varying sizes. Peak broadening is due to both instrumental and structural causes (that depends on the lattice strain and the crystal size).

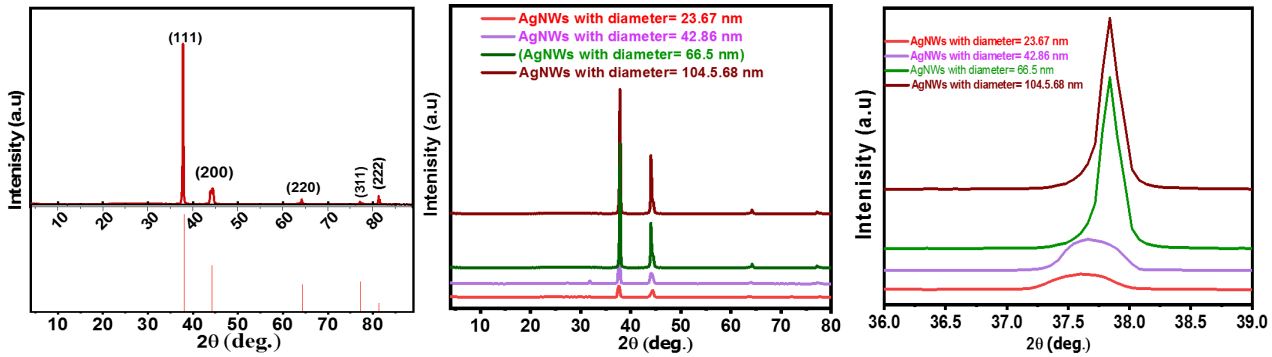

Fig. 1: XRD pattern of AgNWs (a) with reference pattern, (b) corresponding SEM image, (c) XRD patterns with different diameters and (d) XRD broadening.

3.2 Morphological characterization

SEM is one of the most used tools in scientific research today because of its higher magnification, better depth of focus, higher resolution, and simplicity of sample observation. Fig. 2 shows the SEM of AgNWs with different diameters at 500 nm. Fig. 1(a-d) shows SEM images for AgNWs with different of 23.866 nm, 42.67 nm, 66.5 nm, and 104.5 nm, respectively.

3.3 UV-spectroscopy:

Surface plasmon resonance (SPR) will appear in the UV spectroscopy that depends on the geometry and size of silver nanoparticles [50]. Based on the various SPR bands that appear at different frequencies, ultraviolet absorption can be used to illustrate the shape and size of AgNPs [51]. Fig. 3 shows the UV absorbance peaks of AgNWs as a suspension solution for different diameters of AgNWs. Fig. 3a illustrates that the UV of AgNWs suspension samples with different diameters. The UV peaks were observed at 370nm, 376nm, 383nm, and 389nm for corresponding AgNWs with average diameters 23.866 nm, 42.67 nm, 66.5 nm, and 104.5 nm, respectively. It is clear that by increasing the wire diameter, the UV absorption peaks will

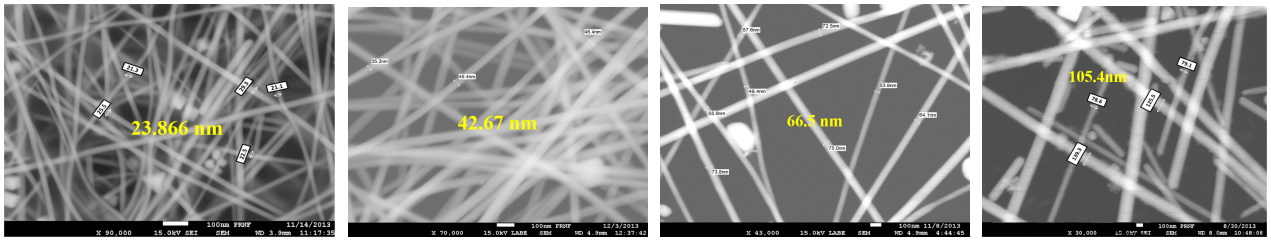

(a) (b) (c) (d)

Fig. 2 SEM images of AgNWs with different diameters.

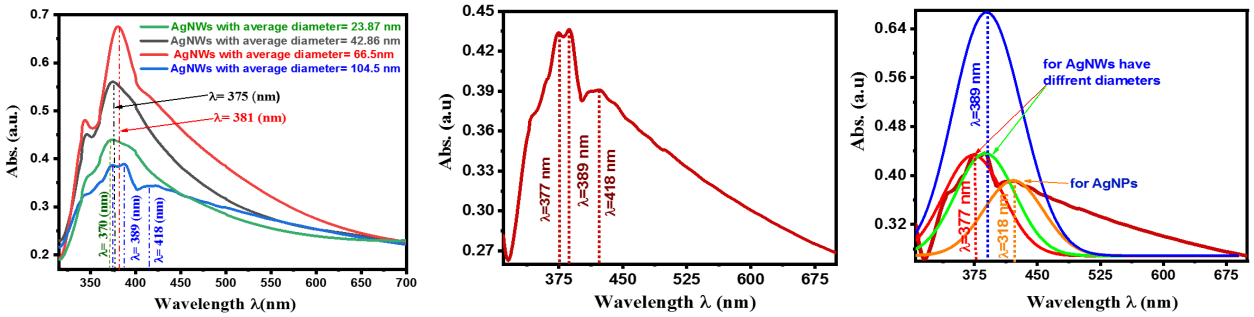

(a) (b) (c)

Fig. 3 UV-visible spectroscopy of synthesized AgNWs (a) average diameters 23.87nm, 42.78 nm,66.5 nm and 105.4 nm and (b and c) with average diameter 105.4nm (polydisperse sample) and the corresponding Gaussian fitting, respectively.

be going to a higher wavelength (red shift) and this is in agreement with the previous research [40, 41, 52-54]. Fig. 3b illustrates the UV absorbance spectra of polydisperse AgNWs suspension with an average diameter of 105.4 nm. Three were observed, two of them had a Plasmon beak at 377 and 389 crossponding to AgNWs while the third peak at 418 nm is characteristic for AgNPs that usually appears around 420 nm. The corresponding Gaussian fitting of the samples were shown in fig. 3(d).

Table 1. the calculated particle size based on XRD data.

AgNWs Diameter (nm)	Pos. [°2Th.]	FWHM [°2Th.] x 10^{-3}	d-spacing [Å] x 10^{-3}	Particle size calculated L_{ave} (nm)
105.4	37.9 ±0.76	0.24 ±4.7	2.38 ±47. 5	40.5 ±0.81
	44.1 ±0.89	0.18 ±3.5	2.10 ±41. 1	55.2 ±1.10
	44.6 ±0.894	0.18 ±3.5	2.03 ±40. 7	55.3 ±1.11
	64.2 ±1.28	0.18 ±3.5	1.45 ±29. 0	60.4 ±1.21
	77.1 ±1.54	0.2 ±4.0	1.24 ±24. 7	57.6 ±1.15
66.5	48.1 ±0.96	0.32 ±6.5	1.24 ±24.	30.7 ±0.61
	59.7 ±1.19	0.22 ±4.5	1.89 ±37. 8	46.8 ±0.94
	62.2 ±1.24	0.22 ±4.4	1.55 ±31. 0	47.3 ±0.95
	65.0 ±1.30	0.23 ±4.8	1.49 ±29. 8	45.0 ±0.90
	76.7 ±1.53	0.24 ±4.8	1.43 ±28. 7	47.7 ±0.95
42.67	37.6 ±0.75	0.47 ±9.4	2.39 ±47. 9	20.3 ±0.41
	43.9 ±0.87	0.41 ±8.3	2.06 ±41. 2	15.8 ±0.32
	44.4 ±0.88	0.30 ±5.9	2.04 ±40. 8	33.1 ±0.66
	64.1 ±1.28	0.65 ±1.3	1.45 ±29. 1	16.5 ±0.33
	72.1 ±1.44	0.71 ±1.4	1.31 ±26. 2	23.6 ±0.47
23.9	37.45±0.75	0.48±9.6	1.93±38	19.77±0.39
	44.95±0.89	0.43±8.6	1.89±37. 8	22.8±0.46
	44.1±0.88	0.30±6.0	1.88± 37	32.46±0.65
	64.83±1.29	0.65±1.3	1.51±3.02	16.00±0.32
	76.97±1.54	0.76±1.5	1.33±18.8	15.19±0.30

3.4 Performance of AgNWs-TCF:

The design of good flexible conductive transparent electrodes has attracted the attention of a lot of scientists and researchers in recent days. Transparent conductive electrodes with high performance should have excellent electrical conductivity, high optical clarity, good mechanical properties, and flexibility. These properties can be obtained by raising the aspect ratio of silver nanowires.

Fig. 4. shows optical properties of the designed AgNWs-TCFs that were prepared by adding 2 mg.mL^{-1} of different AgNWs diameters suspension to a glass substates. Fig. 4a shows the relation between AgNWs-TCFs diameter and light transmittance. The calculated values of transmittance were 93.9 %, 91.5%, 86.7% and 77.6% corresponding to AgNWs-TCFs with diameters 23.866 nm, 42.67 nm, 66.5 nm, and 104.5 nm, respectively. An inverse relation between light transmittance and wires diameter was obtained. The inverse relation could be attributed to the fact that small diameter AgNWs leads to the formation of a small layer thickness than AgNWs with thicker diameter, and, the increase in light scattering with thicker AgNWs. It has been reported that as the diameter of nanowires

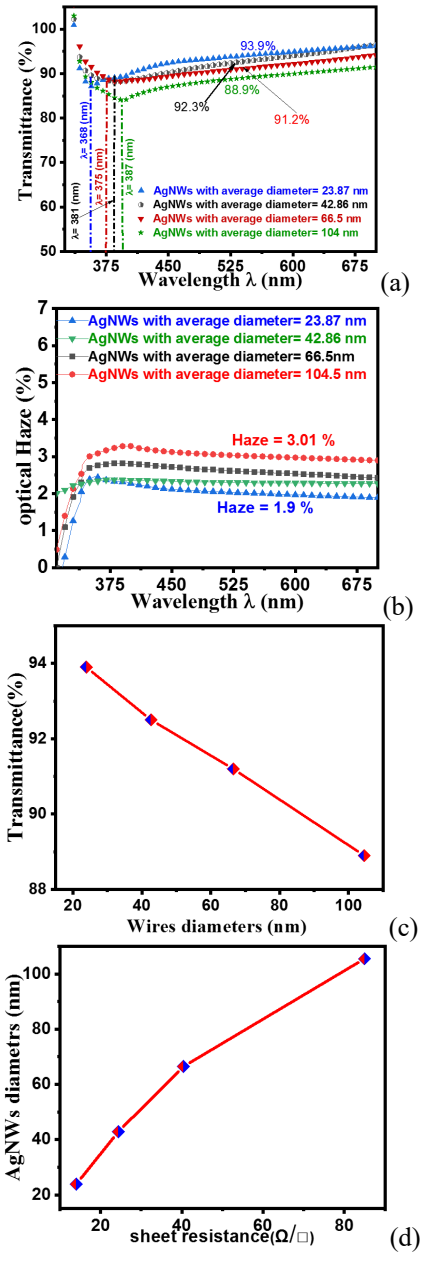

Fig. 4: AgNWs-TCFs prepared with different diameters from 3mg.mL^{-1} AgNWs suspension (a) Transmittance (at λ= 550 nm), (b) optical haze, (c) Transmittance vs AgNWs diameters, (d) sheet resistance vis AgNWs diameters.

increases from 10 nanometers to 100 nanometers, the efficiency of nanowires to block light increases rapidly from 3% to 147% [55]. Transmittance peaks had been observed at wavelengths of 368 nm, 375 nm, 381 nm, and 387 nm for AgNWs with average diameters 23.866 nm, 42.67 nm, 66.5 nm, and 104.5 nm, respectively. The peak positions of the AgNWs coated sample showed the same trend as the AgNWs suspension samples but at lower wavelengths compared to the AgNWs suspension sample and this trend is in agreement the previous study [40].

Consequently, optical haze and AgNWs relation were displayed in fig. 4b. Optical haze depends on the optical transparency, and it was calculated according to the following equation:

$$\text{Haze\%} = \frac{Td}{Tt} * 100, \quad (5)$$

Where *Tt* The total transmittance and *Td* the diffuse Transmittance where, *Tt* is calculated according to the following equation:

$$\text{T}t = \frac{T2}{T1}, \quad (6)$$

Where *T1* is the incident the transmitted light, *T2* is the light transmitted from the sample, while (*Td*) is given by equation (7):

$$\text{Td} = \frac{T4 - T3\ (\frac{T2}{T1})}{T1}, \quad (7)$$

Where *T3* is the light scattered by the instrument and *T4* is the total light scattered by the sample and the instrument together. The final relation of calculated haze is given by equation (8): [56]:

$$\text{Haze\%} = \frac{T4}{T2} - \frac{T3}{T1} \quad (8)$$

Fig. 4b shows the optical haze of AgNWs with different diameters. optical hazes were found have values of 1.9 %, 2.7%, 3% and 3.4% for the corresponding AgNWs- TCFs with diameters 23.866 nm, 42.67 nm, 66.5 nm, and 104.5 nm, respectively. As was expected the haze value will increase with increasing the wire diameter [57].

Fig. 4c summarizes the relationship between light transmittance and wire diameters. The figure exhibits that light transmittance is inversely proportional to the wire diameters as mentioned previously. Also, the relation between the sheet resistance of the AgNWs-TCFs which were designed by 3 mg. mL^{-1} AgNWs suspension ink and AgNWs diameters were shown in fig. 4d. It can be concluded that AgNWs-TCFs which were designed by the from AgNWs with a small diameter exhibited higher transparency and lower haze than those designed by using AgNWs with higher diameters. [57].

Fig. 5 shows AgNWs suspension ink used for coating glass substrates and different AgNWs-TCFs. 10 mg.ml^{-1} AgNWs suspension ink with an average diameter of 23.87nm was shown in fig. 5a. Fig. 5b shows the AgNWs-TCF which was designed by adding 3 mg.mL^{-1} suspension ink with measured resistivity of 14 ohm/seq. Consequently, fig. 5c shows a photographic image for different AgNWs-TCFs made with AgNWs suspension ink of 23.78nm diameter but with different concentrations of 2 mg.mL^{-1}, 3 mg.mL^{-1}, 4 mg.mL^{-1} and 5mg.mL^{-1} and their crossponding sheet resistances. highly transparent and homogeneous films were obtained as shown in fig. 5c. Also as was expected the lowest sheet resistance of 2.3 ohm associated with less clarity was observed for the AgNWs-TCFs designed with concentrated AgNWs suspension of 5mg.mL^{-1}.


(a)

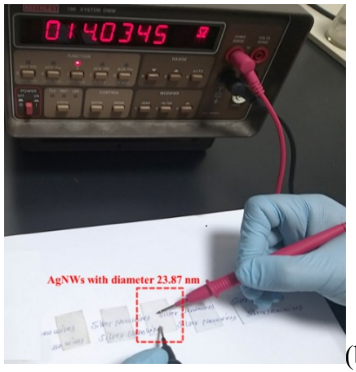

(b)

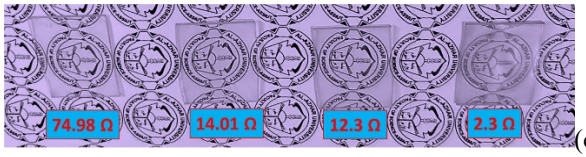

(c)

Fig. 5: AgNWs with average diameter 23.78 nm and its transparent conductive films: (a) 10 mg.mL-1 AgNWs suspension ink, (b) image of measured sheet and (c) image of AgNWs -TCFs coated by AgNWs with diameter 23.78 nm with different AgNWs concentrations.

Fig. 6a show the transmittance of different AgNWs-TCFs made with an average diameter of 23.78 nm but with different AgNWs ink concentrations. Transmittance values of 93.9%, 91.5%, 87.9% and 81.3% were observed which are corresponding to AgNWs suspension inks of 2 mg.mL^{-1}, 3 mg.mL^{-1}, 4 mg.mL^{-1} and 5 mg.mL^{-1} respectively. Increasing of ink concentration will lead to a reduction of transmittance peak, which is attributed to the increasing of thin-film thickness and accordingly, as the layer gets thicker it will block the light coming through.

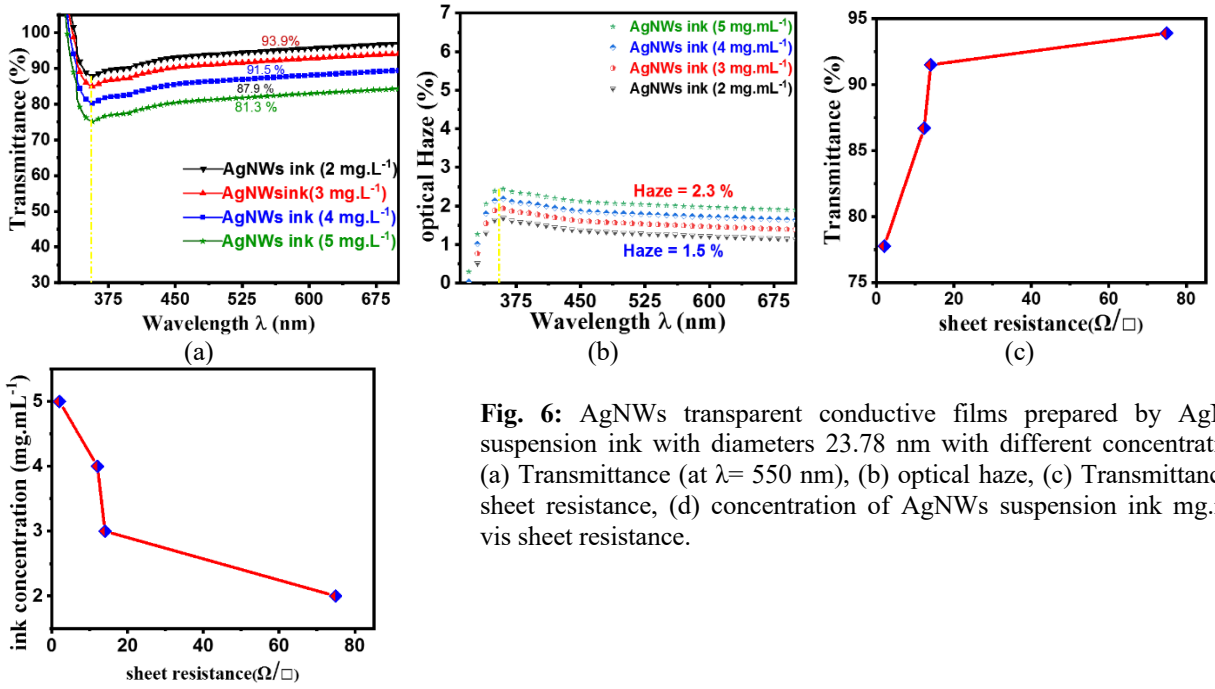

Fig. 6: AgNWs transparent conductive films prepared by AgNWs suspension ink with diameters 23.78 nm with different concentrations; (a) Transmittance (at λ= 550 nm), (b) optical haze, (c) Transmittance vs sheet resistance, (d) concentration of AgNWs suspension ink mg.mL^{-1} vis sheet resistance.

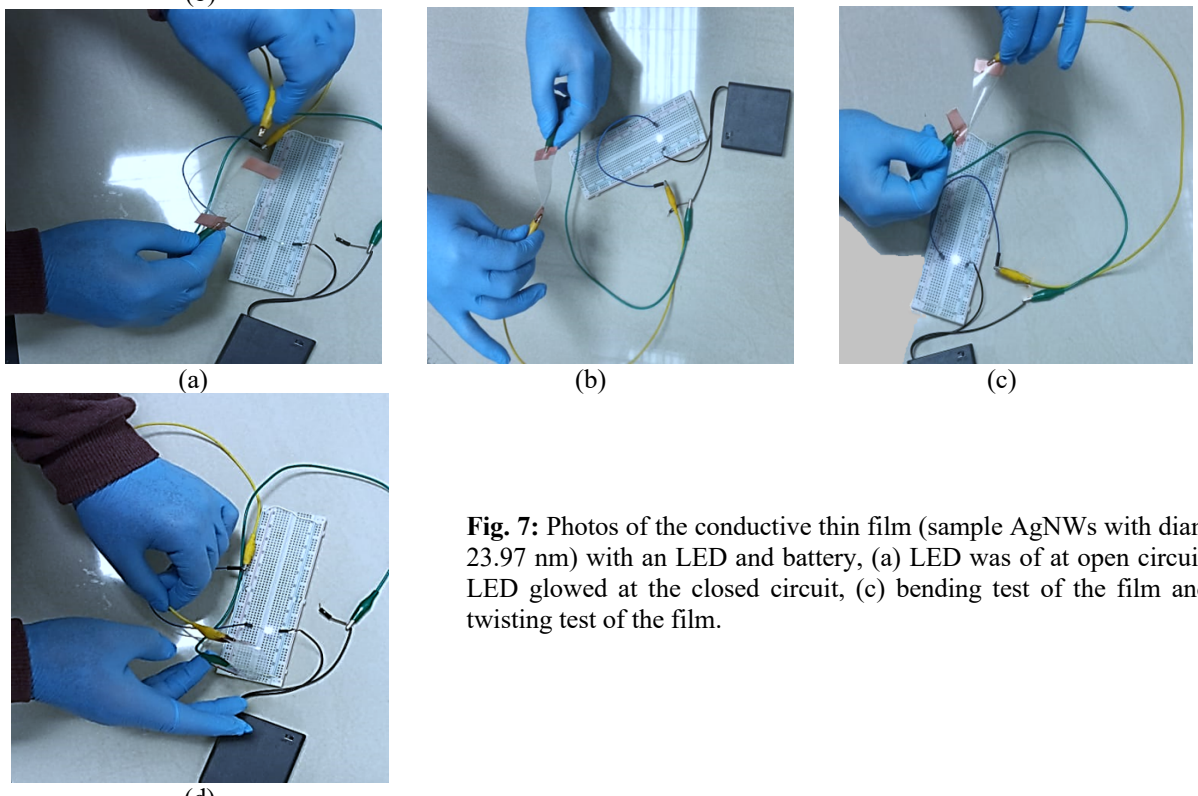

Fig. 7: Photos of the conductive thin film (sample AgNWs with diameter 23.97 nm) with an LED and battery, (a) LED was of at open circuit, (b) LED glowed at the closed circuit, (c) bending test of the film and (d) twisting test of the film.

In addition, fig. 6b shows the relation between the optical haze and different AgNWs-TCFs. Optical haze values were found to have a direct relation with AgNWs suspension ink concentration. Fig. 6(b,c) shows the relation between transmittance and AgNWs suspension concentration with sheet resistance for AgNWs-TCFs prepared by different AgNWs suspension ink with an average diameter of 23.78. sheet resistance values were found to be 74.87Ω, 14.03 Ω, 12.01 Ω and 2 Ω for the corresponding transmittance of 93.9%, 91.5%, 87.9 and 81.3% respectively (fig. 6c). Similarly, fig. 6d indicated that the sheet resistance values were inversely proportion to AgNWs ink concentrations.

3.5 Flexible AgNWs-TCFs:

The flexibility of the AgNWs-TCF was studied by connecting it to a small LED and a battery. At both ends of the film, thin copper foils are used as electrodes and were glued on the top of the AgNWs-TCF layer. Flexible AgNWs-TCFs are shown in fig. 7. The Figures indicated usability of AgNWs-TCFs as a flexible and conductive electrode. The bending or twisting were made for the same electrode up to 100 times in this test with no apparent change in both optical and electrical properties were observed. These results look promising for the application of flexible AgNWs in future applications.

4. Conclusion

The current reperch used polyol technique to synthesize silver nanowires with excellent uniformity and controllable size. AgNWs morphology was characterized by SEM and XRD. Optical characterization had been done and it was found that a redshift in the absorbance spectra was observed by increasing the wire diameter at the same time the electrical conductivity was found to increase with the increasing of wire diameters. Accordingly, the best optical and electrical properties was obtained with AgNWs have average diameter of 23.87nm. The fabrication of AgNWs thin film had been done successfully with good homogeneity, high transparency excellent electrical conductivity. Optimum condition for Spin coater was adjusted to coat AgNWs on glass substrates, whereas AgNWs were coated on PET by using Meyer rods. AgNWs-TCFs were obtained with high flexibility and high transparency (91%, low sheet resistance (14.3 Ω/□) and optical haze less than 2%. The properties of the designed AgNWs-TCF., met the requirements for the manufacture of future flexible optoelectronic and sensor equipment.

Conflict of Interest

All authors declare that there is no conflict of interest regarding the publication of this paper.

References

[1] B. Han, K. Pei, Y. Huang, X. Zhang, Q. Rong, Q. Lin, *et al.*, "Uniform self-forming metallic network as a high-performance transparent conductive electrode," *Advanced materials,* vol. 26, pp. 873-877, 2014.

[2] J. Krantz, M. Richter, S. Spallek, E. Spiecker, and C. J. Brabec, "Solution-processed metallic nanowire electrodes as indium tin oxide replacement for thin-film solar cells," *Advanced Functional Materials,* vol. 21, pp. 4784-4787, 2011.

[3] J. Jiu and K. Suganuma, "Metallic nanowires and their application," *IEEE Transactions on Components, Packaging and Manufacturing Technology,* vol. 6, pp. 1733-1751, 2016.

[4] R. E. Triambulo, J.-H. Kim, and J.-W. Park, "Highly flexible organic light-emitting diodes on patterned Ag nanowire network transparent electrodes," *Organic Electronics,* vol. 71, pp. 220-226, 2019.

[5] A. Tolcin, "Mineral Commodity Summaries-Indium," *US Geological Survey. Version,* 2008.

[6] S. C. Mannsfeld, B. C. Tee, R. M. Stoltenberg, C. V. H. Chen, S. Barman, B. V. Muir, *et al.*, "Highly sensitive flexible pressure sensors with microstructured rubber dielectric layers," *Nature materials,* vol. 9, pp. 859-864, 2010.

[7] T. Sekitani, H. Nakajima, H. Maeda, T. Fukushima, T. Aida, K. Hata, *et al.*, "Stretchable active-matrix organic light-emitting diode display using printable elastic conductors," *Nature materials,* vol. 8, pp. 494-499, 2009.

[8] W. Gaynor, J.-Y. Lee, and P. Peumans, "Fully solution-processed inverted polymer solar cells with laminated nanowire electrodes," *ACS nano,* vol. 4, pp. 30-34, 2010.

[9] X. Ho, L. Ye, S. V. Rotkin, Q. Cao, S. Unarunotai, S. Salamat, *et al.*, "Scaling properties in transistors that use aligned arrays of single-walled carbon nanotubes," *Nano letters,* vol. 10, pp. 499-503, 2010.

[10] H. Kang, S. Jung, S. Jeong, G. Kim, and K. Lee, "Polymer-metal hybrid transparent electrodes for flexible electronics," *Nat Commun,* vol. 6, p. 6503, Mar 19 2015.

[11] T. Ebbesen, H. Lezec, H. Hiura, J. Bennett, H. Ghaemi, and T. Thio, "Electrical conductivity of individual carbon nanotubes," *Nature,* vol. 382, pp. 54-56, 1996.

[12] J.-Y. Lee, S. T. Connor, Y. Cui, and P. Peumans, "Solution-processed metal nanowire mesh transparent electrodes," *Nano letters,* vol. 8, pp. 689-692, 2008.

[13] C. Kang, S. Yang, M. Tan, C. Wei, Q. Liu, J. Fang, *et al.*, "Purification of Copper Nanowires to Prepare Flexible Transparent Conductive Films with High Performance," *ACS Applied Nano Materials,* vol. 1, pp. 3155-3163, 2018/07/27 2018.

[14] L. Zhao, S. Yu, X. Li, M. Wu, and L. Li, "High-performance flexible transparent conductive films based on copper nanowires with electroplating welded junctions," *Solar Energy Materials and Solar Cells,* vol. 201, p. 110067, 2019/10/01/ 2019.

[15] V. B. Nam and D. Lee, "Copper Nanowires and Their Applications for Flexible, Transparent Conducting Films: A Review," *Nanomaterials,* vol. 6, 2016.

[16] X. Y. Zeng, Q. K. Zhang, R. M. Yu, and C. Z. Lu, "A new transparent conductor: silver nanowire film buried at the surface of a transparent polymer," *Advanced materials,* vol. 22, pp. 4484-4488, 2010.

[17] D. S. Leem, A. Edwards, M. Faist, J. Nelson, D. D. Bradley, and J. C. De Mello, "Efficient organic solar cells with

solution-processed silver nanowire electrodes," *Advanced materials,* vol. 23, pp. 4371-4375, 2011.
[18] S. De, T. M. Higgins, P. E. Lyons, E. M. Doherty, P. N. Nirmalraj, W. J. Blau*, et al.*, "Silver nanowire networks as flexible, transparent, conducting films: extremely high DC to optical conductivity ratios," *ACS nano,* vol. 3, pp. 1767-1774, 2009.
[19] L. Hu, H. S. Kim, J.-Y. Lee, P. Peumans, and Y. Cui, "Scalable coating and properties of transparent, flexible, silver nanowire electrodes," *ACS nano,* vol. 4, pp. 2955-2963, 2010.
[20] Y. Jin, Y. Sun, K. Wang, Y. Chen, Z. Liang, Y. Xu*, et al.*, "Long-term stable silver nanowire transparent composite as bottom electrode for perovskite solar cells," *Nano Research,* vol. 11, pp. 1998-2011, 2018.
[21] J.-J. Chen, S.-L. Liu, H.-B. Wu, E. Sowade, R. R. Baumann, Y. Wang*, et al.*, "Structural regulation of silver nanowires and their application in flexible electronic thin films," *Materials & Design,* vol. 154, pp. 266-274, 2018.
[22] Y. J. Jo, C. Kim, J. H. Lee, M. S. Ko, A. Jo, J.-Y. Kim*, et al.*, "Development of patterned 1D metal nanowires with adhesion layer for mesh electrodes of flexible transparent conductive films for touch screen panels," *Journal of Nanoscience and Nanotechnology,* vol. 16, pp. 11586-11590, 2016.
[23] H. Peng, H. Jiang, S. Tu, S. Zhang, E. Ren, B. Yan*, et al.*, "High-performance and ultraflexible PEDOT/silver nanowires/graphene films for electrochromic applications," *Optics letters,* vol. 45, pp. 2443-2446, 2020.
[24] T. Guan, L. Fang, L. Liu, F. Wu, Y. Lu, H. Luo*, et al.*, "Self-supported ultrathin NiCo-LDH nanosheet array/Ag nanowire binder-free composite electrode for high-performance supercapacitor," *Journal of Alloys and Compounds,* vol. 799, pp. 521-528, 2019.
[25] C. Liang, K. Ruan, Y. Zhang, and J. Gu, "Multifunctional flexible electromagnetic interference shielding silver nanowires/cellulose films with excellent thermal management and joule heating performances," *ACS applied materials & interfaces,* vol. 12, pp. 18023-18031, 2020.
[26] L. Meng, R. Bian, C. Guo, B. Xu, H. Liu, and L. Jiang, "Aligning Ag nanowires by a facile bioinspired directional liquid transfer: toward anisotropic flexible conductive electrodes," *Advanced Materials,* vol. 30, p. 1706938, 2018.
[27] M. Kumar, J. Kim, and C.-P. Wong, "Transparent and flexible photonic artificial synapse with piezo-phototronic modulator: Versatile memory capability and higher order learning algorithm," *Nano Energy,* vol. 63, p. 103843, 2019.
[28] X. Liu, R. Wang, Y. He, Z. Ni, N. Su, R. Guo*, et al.*, "Construction of alternating layered quasi-three-dimensional electrode Ag NWs/CoO for water splitting: A discussion of catalytic mechanism," *Electrochimica Acta,* vol. 317, pp. 468-477, 2019.
[29] Y. A. Attia and S. H. Abdel-Hafez, "Reusable photoresponsive Ag/AgCl nanocube-catalyzed one-pot synthesis of seleno [2, 3-b] pyridine derivatives," *Research on Chemical Intermediates,* vol. 46, pp. 3165-3177, 2020.
[30] D. Chen, X. Qiao, X. Qiu, J. Chen, and R. Jiang, "Convenient synthesis of silver nanowires with adjustable diameters via a solvothermal method," *Journal of Colloid and Interface Science,* vol. 344, pp. 286-291, 2010.
[31] K. Zhao, Q. Chang, X. Chen, B. Zhang, and J. Liu, "Synthesis and application of DNA-templated silver nanowires for ammonia gas sensing," *Materials Science and Engineering: C,* vol. 29, pp. 1191-1195, 2009.
[32] D. Zhang, L. Qi, J. Yang, J. Ma, H. Cheng, and L. Huang, "Wet chemical synthesis of silver nanowire thin films at ambient temperature," *Chemistry of Materials,* vol. 16, pp. 872-876, 2004.
[33] B. S. Kim, J. B. Pyo, J. G. Son, G. Zi, S.-S. Lee, J. H. Park*, et al.*, "Biaxial stretchability and transparency of Ag nanowire 2D mass-spring networks prepared by floating compression," *ACS applied materials & interfaces,* vol. 9, pp. 10865-10873, 2017.
[34] F. Fievet, J. Lagier, B. Blin, B. Beaudoin, and M. Figlarz, "Homogeneous and heterogeneous nucleations in the polyol process for the preparation of micron and submicron size metal particles," *Solid State Ionics,* vol. 32, pp. 198-205, 1989.
[35] T. N. Trung, V. K. Arepalli, R. Gudala, and E.-T. Kim, "Polyol synthesis of ultrathin and high-aspect-ratio Ag nanowires for transparent conductive films," *Materials Letters,* vol. 194, pp. 66-69, 2017.
[36] M. B. Gebeyehu, T. F. Chala, S.-Y. Chang, C.-M. Wu, and J.-Y. Lee, "Synthesis and highly effective purification of silver nanowires to enhance transmittance at low sheet resistance with simple polyol and scalable selective precipitation method," *RSC advances,* vol. 7, pp. 16139-16148, 2017.
[37] A. Nekahi, S. Marashi, and D. H. Fatmesari, "High yield polyol synthesis of round-and sharp-end silver nanowires with high aspect ratio," *Materials Chemistry and Physics,* vol. 184, pp. 130-137, 2016.
[38] K. E. Korte, S. E. Skrabalak, and Y. Xia, "Rapid synthesis of silver nanowires through a CuCl-or CuCl 2-mediated polyol process," *Journal of Materials Chemistry,* vol. 18, pp. 437-441, 2008.
[39] A. Alsayed, A. Ahmed, C. Badre, L. A. Hough, and C. A. S. Burel, " PROCESSES FOR MAKING SILVER MACROSTRUCTURE," US 010130992 B 2 Patent, Nov. 20, 2018.
[40] R. D. Abdel-Rahim, A. M. Nagiub, O. A. Pharghaly, M. A. Taher, E. S. Yousef, and E. R. shaaban, "Optical properties for flexible and transparent silver nanowires electrodes with different diameters," *Optical Materials,* vol. 117, p. 111123, 2021/07/01/ 2021.
[41] R. D. Abdel-Rahim, M. Y. Emran, A. M. Nagiub, O. A. Farghaly, and M. A. Taher, "Silver nanowire size-dependent effect on the catalytic activity and potential sensing of H2O2," *Electrochemical Science Advances,* vol. 1, p. e2000031, 2021.
[42] M. R. Johan, N. A. K. Aznan, S. T. Yee, I. H. Ho, S. W. Ooi, N. Darman Singho*, et al.*, "Synthesis and growth mechanism of silver nanowires through different mediated agents (CuCl2 and NaCl) polyol process," *Journal of Nanomaterials,* vol. 2014, 2014.
[43] M. Bobinger, V. Dergianlis, M. Becherer, and P. Lugli, "Comprehensive Synthesis Study of Well-Dispersed and Solution-Processed Metal Nanowires for Transparent Heaters," *Journal of Nanomaterials,* vol. 2018, pp. 1-13, 2018.
[44] H. Mao, J. Feng, X. Ma, C. Wu, and X. Zhao, "One-dimensional silver nanowires synthesized by self-seeding polyol process," *Journal of nanoparticle research,* vol. 14, p. 887, 2012.
[45] A. R. Siekkinen, J. M. McLellan, J. Chen, and Y. Xia, "Rapid synthesis of small silver nanocubes by mediating polyol

reduction with a trace amount of sodium sulfide or sodium hydrosulfide," *Chemical physics letters,* vol. 432, pp. 491-496, 2006.
[46] X.-s. Yan, P. Lin, X. Qi, and L. Yang, "Finnis–Sinclair potentials for fcc Au–Pd and Ag–Pt alloys," *International Journal of Materials Research,* vol. 102, pp. 381-388, 2011.
[47] M. Shkir, M. T. Khan, I. Ashraf, S. AlFaify, A. M. El-Toni, A. Aldalbahi*, et al.*, "Rapid microwave-assisted synthesis of Ag-doped PbS nanoparticles for optoelectronic applications," *Ceramics International,* vol. 45, pp. 21975-21985, 2019.
[48] C. Jia, P. Yang, and A. Zhang, "Glycerol and ethylene glycol co-mediated synthesis of uniform multiple crystalline silver nanowires," *Materials Chemistry and Physics,* vol. 143, pp. 794-800, 2014.
[49] J. Ajuria, I. Ugarte, W. Cambarau, I. Etxebarria, R. Tena-Zaera, and R. Pacios, "Insights on the working principles of flexible and efficient ITO-free organic solar cells based on solution processed Ag nanowire electrodes," *Solar energy materials and solar cells,* vol. 102, pp. 148-152, 2012.
[50] J. P. Kottmann, O. J. Martin, D. R. Smith, and S. Schultz, "Plasmon resonances of silver nanowires with a nonregular cross section," *Physical Review B,* vol. 64, p. 235402, 2001.
[51] Y. Sun and Y. Xia, "Gold and silver nanoparticles: a class of chromophores with colors tunable in the range from 400 to 750 nm," *Analyst,* vol. 128, pp. 686-691, 2003.
[52] E.-J. Lee, M.-H. Chang, Y.-S. Kim, and J.-Y. Kim, "High-pressure polyol synthesis of ultrathin silver nanowires: Electrical and optical properties," *Apl materials,* vol. 1, p. 042118, 2013.
[53] R.-L. Zong, J. Zhou, Q. Li, B. Du, B. Li, M. Fu*, et al.*, "Synthesis and optical properties of silver nanowire arrays embedded in anodic alumina membrane," *The Journal of Physical Chemistry B,* vol. 108, pp. 16713-16716, 2004.
[54] Y. Sun, B. Gates, B. Mayers, and Y. Xia, "Crystalline silver nanowires by soft solution processing," *Nano letters,* vol. 2, pp. 165-168, 2002.
[55] S. M. Bergin, Y.-H. Chen, A. R. Rathmell, P. Charbonneau, Z.-Y. Li, and B. J. Wiley, "The effect of nanowire length and diameter on the properties of transparent, conducting nanowire films," *Nanoscale,* vol. 4, pp. 1996-2004, 2012.
[56] C. Preston, Y. Xu, X. Han, J. N. Munday, and L. Hu, "Optical haze of transparent and conductive silver nanowire films," *Nano Research,* vol. 6, pp. 461-468, 2013.
[57] Y. Liu, Y. Chen, R. Shi, L. Cao, Z. Wang, T. Sun*, et al.*, "High-yield and rapid synthesis of ultrathin silver nanowires for low-haze transparent conductors," *RSC advances,* vol. 7, pp. 4891-4895, 2017.